1521-0111/87/3/501–512$25.00
MOLECULAR PHARMACOLOGY

http://dx.doi.org/10.1124/mol.114.096941
Mol Pharmacol 87:501–512, March 2015

Repurposing the Antipsychotic Trifluoperazine as an Antimetastasis Agent

Ashleigh Pulkoski-Gross, Jian Li, Carolina Zheng, Yiyi Li, Nengtai Ouyang, Basil Rigas, Stanley Zucker, and Jian Cao

Department of Pharmacological Sciences/Cancer Prevention (A.P.G.), Department of Medicine/Cancer Prevention (C.Z., Y.L., B.R., J.C.), and Department of Medicine/Hematology & Oncology (S.Z.), Stony Brook University, Stony Brook, New York; Jimei University, Xiamen, China (J.L.); and Department of Pathology, Sun Yat-Sen Memorial Hospital, Sun Yat-Sen University, China (N.O.)

Received November 18, 2014; accepted December 31, 2014

ABSTRACT

Because cancer cell invasion is a critical determinant of metastasis, targeting invasion is a viable approach to prevent metastasis. Utilizing a novel three-dimensional high-throughput invasion assay, we screened a National Cancer Institute compound library and discovered compounds demonstrating inhibitory effects on cancer cell invasion. One hit, trifluoperazine, suppresses invasion of human cancer cell lines while displaying a limited cytotoxicity profile. This inhibition is due to the interference with cancer cell migratory ability but not proteolytic activity. Treatment of cancer cells with trifluoperazine significantly reduces angiogenesis and prevents cancer cell invasion through a chorioallantoic basement membrane. Mechanistically, treatment results in decreased phosphorylated AKT (Ser^{473} and Thr^{308}) and β-catenin (Ser^{552}). Lack of phosphorylation of Ser^{552} of β-catenin prevents β-catenin nuclear relocation, resulting in decreased expression of vascular endothelial growth factor, likely mediated through dopamine receptor D2. Taken together, we demonstrated that trifluoperazine is responsible for reducing the angiogenic and invasive potential of aggressive cancer cells through dopamine receptor D2 to modulate the β-catenin pathway and propose that trifluoperazine may be used as an antimetastasis chemotherapeutic.

Introduction

Malignant tumors are largely considered incurable and those without evidence of dissemination will frequently relapse (Redig and McAllister, 2013), as they often harbor micrometastases that are not apparent at the time of diagnosis (Talmadge and Fidler, 2010). Accordingly, patients have a high mortality rate and approximately 90% of cancer patients succumb to the disease because of metastasis, even with early detection (Leaf and Burke, 2004). Treatments designed to target primary tumors, such as surgery, radiotherapy, and chemotherapy in refractory types of cancer are ineffective in eradicating disseminated cancers (Norton and Massague, 2006). Hence, there is an unmet need to identify agents capable of inhibiting metastasis.

A strategy to combat metastasis includes pursuing drug development for compounds that can attenuate cell invasion, as it is a critical early step in the complex metastatic cascade (Hanahan and Weinberg, 2011). The metastatic process was long considered a unidirectional event, with cells leaving the primary tumor at early stages of disease and colonizing distant organs. The course of metastasis has been redefined to include not only the distribution of cancer cells to secondary organs but also the reseeding and perpetuation of the established tumors by circulating cancer cells (Norton and Massague, 2006; Comen and Norton, 2012). Because circulating tumor cells that have escaped from the primary tumor can reseed tumor cells at the primary site and contribute to secondary lesions (Kim et al., 2009), identifying novel compounds capable of inhibiting cancer invasion provides an effective strategy for all stages of the disease.

Although it is clear that metastasis is often the reason for treatment failure, it is generally not an endpoint that is taken into consideration when initially evaluating anticancer drugs. Cancer drug development has traditionally focused on identifying antimitotic and cytotoxic compounds; drugs with selective antimetastatic effects have not been identified. This is mostly due to the fact that cancer metastasis is a complex cascade and there has been a lack of effective tools for studying metastasis. For many types of solid cancers, drugs that have been developed to suppress cancer cell proliferation are capable of prolonging patient survival but are not likely to improve a person's chances of survival. The key to improving patient

This work was supported in part by the Baldwin Breast Cancer Foundation and National Cancer Institute [1R01CA166936 to J.C.] and the United States Army Medical Research Acquisition Activity award [W81XWH10-1-0873 to B.R.].
dx.doi.org/10.1124/mol.114.096941.

ABBREVIATIONS: aiRNA, asymmetric interfering RNA; CAM, chorioallantoic membrane; CSC, cancer stem-like cells; DMSO, dimethylsulfoxide; ELISA, enzyme-linked immunosorbent assay; EMT, epithelial-to-mesenchymal transition; FDA, Food and Drug Administration; HUVEC, human umbilical vein endothelial cells; MMP, matrix metalloproteinase; MTT, 3-(4,5-dimethylthiazol-2-yl)-2,5-diphenyltetrazolium bromide; PBS, phosphate-buffered saline; PI, propidium iodide; RT-PCR, reverse-transcription polymerase chain reaction; TFP, trifluoperazine; VEGF, vascular endothelial growth factor.

survival is stopping metastases, which accounts for 90% of treatment failure among all cancers (Leaf and Burke, 2004).

To address the lack of effective drugs targeting cancer metastasis, we employed our novel three-dimensional high-throughput assay (Evensen et al., 2013) to identify potential agents targeting cancer cell invasion. Screening drugs in vitro against cancer cells has historically been done in a two-dimensional format, assaying cells on a flat surface for proliferation and/or cytotoxicity. Monitoring the effects of anticancer agents on cancer cells in two-dimensional cultures, however, may lead to false positives. It has been demonstrated that the phenotype of a cell tethered to a two-dimensional surface as compared with being embedded in a three-dimensional matrix can be vastly different (Bissell et al., 1999; Bissell and Radisky, 2001; Anders et al., 2003). These differences lie in receptor expression, extracellular matrix deposition, and metabolism and contribute to altered responses of cells to treatment. Over 700 different genes have documented changes in expression in three-dimensional culture compared with two-dimensional culture (Horning et al., 2008). Cells grown in three-dimensional cultures also demonstrate a decrease in drug uptake and an extended time to drug uptake from the environment, leading to the conclusion that tumor architecture influences drug efficacy (Horning et al., 2008). Three-dimensional culture better recapitulates tumor structure; therefore, employing a three-dimensional high-throughput assay facilitates identification of drugs more likely to be effective in vivo (Horning et al., 2008).

Herein, we used our three-dimensional high-throughput assay to screen a National Cancer Institute Diversity compound library against invasive cancer cells. One of the hits, a clinically-used antidepressant drug trifluoperazine (TFP), was found to reduce cancer cell invasion in the three-dimensional environment without notable cytotoxicity. TFP reduced levels of phosphorylated AKT and β-catenin and the reduction in the activity of these proteins results in decreased invasive behavior and angiogenic potential. Knockdown of the TFP target dopamine receptor D_2 (DRD2) recapitulates the reduction in p-β-catenin and p-AKT, suggesting that the ability of TFP to reduce the invasive capacity of cancer cells lies in its ability to target the dopamine receptor. Our study demonstrates for the first time that TFP may have a new use in preventing cancer metastasis.

Materials and Methods

Collagen Type I (acetic acid-extracted native type I collagen from rat tail tendon), Matrigel, and propidium iodide (PI) were obtained from BD Bioscience Discovery Labware (Franklin Lakes, NJ). Diversity Set II compound library was obtained from the Developmental Therapeutics Program in the National Cancer Institute/National Institutes of Health (Bethesda, MD). Hoechst nuclear stain was purchased from Invitrogen (Grand Island, NY). Trifluoperazine hydrochloride and haloperidol were acquired from Sigma-Aldrich (St. Louis, MO). Rabbit anti–p-β-catenin^{Ser552}, anti–β-catenin (total), anti–p-AKT^{Ser473}, anti–p-AKT^{Thr308}, and anti-AKT (total) were all purchased from Cell Signaling Technology (Danvers, MA). Anti-DRD2 antibody was purchased from EMD Biosciences (Billerica, MA). Mouse anti-actin and anti–α/β-tubulin antibodies were purchased from Cell Signaling Technology. Horseradish peroxidase conjugated anti-rabbit and anti-mouse antibodies were obtained from Rockland Immunochemicals (Gilbertsville, PA). Alexa Fluor 568 anti-rabbit antibodies were purchased from Molecular Probes, Life Technologies (Grand Island, NY).

Cell Lines and Treatment of Cells. Cell lines were obtained from the American Type Culture Collection (Manassas, VA). Cell lines used include human prostate cancer PC3 and human metastatic prostate cancer C4-2b, both of which were maintained in RPMI 1640 medium (Corning, Mediatech, Manassas, VA). Human fibrosarcoma HT1080 and murine fibroblasts NIH/3T3 were maintained in Dulbecco's modified Eagle's medium–high glucose medium (Corning, Mediatech); all media were supplemented with 10% fetal bovine serum and 1% penicillin/streptomycin. Human umbilical vein endothelial cells (HUVEC) were maintained in human endothelial serum free media (Gibco, Life Technologies, Norwalk, CT) supplemented with 20% fetal bovine serum, 20 ng/ml basic fibroblast growth factor and 20 ng/ml epidermal growth factor (R&D Systems, Minneapolis, MN). HUVEC were cultured in tissue culture dishes coated with sterile 5% gelatin. All cells were maintained in a humidified environment at 37°C and 5% CO_2 for all experiments.

Three-Dimensional High-Throughput Invasion Assay. The three-dimensional high-throughput invasion assay was performed as previously described (Evensen et al., 2013). Briefly, cells were mixed with 3 mg/ml neutralized type I collagen (1.5 mg/ml final concentration of type I collagen). The mixture was dotted into each well of a 96-well plate and allowed to solidify at 37°C. The cell-matrix dot was then covered with a layer of 1.5 mg/ml neutralized type I collagen. After solidification of cover collagen at 37°C, compounds from the National Cancer Institute library were added at 10 μM, and dimethylsulfoxide (DMSO) was used as a control in complete medium. Incubation was carried out overnight at 37°C and cells were stained with PI and Hoechst.

Cell Viability Assay. HT1080 and NIH/3T3 cells were cultured in complete media with or without TFP. Media and drugs were changed daily, and cell viability was monitored by MTT assay [3-(4,5-dimethylthiazol-2-yl)-2,5-diphenyltetrazolium bromide] (Promega, Madison, WI). Each day, cells were exposed to MTT and incubated at 37°C for 4 hours. The reaction was stopped, and formazan crystals were solubilized; the resultant solution was subject to colorimetric spectrophotometry and read at a wavelength of 570 nm.

Protease Assay. Total proteolytic activity was detected by employing the Fluorescent Detection Kit (Sigma-Aldrich). Cell lysates were incubated overnight at 37°C with a fluorescein-isothiocyanate–labeled casein substrate and subsequently precipitated with trichloroacetic acid. The supernatant was assessed for fluorescence intensity after dilution in assay buffer. Fluorescence was measured using excitation and emission wavelengths of 485 and 535 nm, respectively, on a SpectraMax Gemini EM (Molecular Devices, Sunnyvale, CA) fluorescent plate reader.

Chorioallantoic Membrane Angiogenesis and Invasion Assay. The chorioallantoic membrane (CAM) assay was performed as previously described (Deryugina and Quigley, 2008). Fertilized white chicken eggs (SPF Premium, Charles River Laboratory, North Franklin, CT) were incubated at 37°C in 70% humidity for 3 days. The embryos were then incubated ex ovo in a sterile Petri dish for 7 days. Gelatin sponges adsorbed with HT1080 cells treated with or without TFP were implanted on the CAM surface (Ribatti et al., 2006), and neovasculature was counted on day 4 postimplantation. For histochemical analysis of the chorioallantoic membrane, embryos were treated as for the angiogenesis assay, except at day 10 the embryos were inoculated with pretreated HT1080 cells in a sterile 2-mm ring. After a 4-day incubation, CAM segments containing the ring were formalin fixed and sectioned by microtome into 5-μm sections after paraffin embedding. Sections were then stained with hematoxylin and counterstained with eosin.

Enzyme-Linked Immunosorbent Assay for Vascular Endothelial Growth Factor. Secreted vascular endothelial growth factor (VEGF) was assayed using the R&D Systems Human VEGF DuoSet enzyme-linked immunosorbent assay (ELISA) kit (R&D Systems,). Briefly, HT1080 cells were incubated overnight in the presence or absence of TFP in complete medium, and the medium was then incubated in a 96-well plate that had previously been coated in the VEGF capture antibody and blocked with filtered 1% bovine serum albumin and washed in phosphate-buffered saline (PBS)–Tween (0.05% Tween).

Subsequently, the samples were removed and the plate incubated with the VEGF detection antibody and streptavidin–horseradish peroxidase at the concentrations suggested by the manufacturer, with PBS-Tween washes between each buffer change. 3, 3′,5,5′-Tetramethylbenzidine was used to develop the enzyme-linked immunosorbent assay ELISA, and the optical density was read at 450 nm with a correction wavelength of 540 nm.

Endothelial Cell Network Formation. HUVEC cells were trypsinized and collected. Equivalent numbers of cells were resuspended in media with either DMSO or 2.5 μM TFP. The isolated cells were then placed over a solidified Matrigel coating within the wells of a 48-well tissue culture dish (70,000 cells/well). The cells were allowed to incubate overnight before bright-field imaging using the Nikon Eclipse TE2000-S (Tokyo, Japan) equipped with a Sutter Instruments Smart-Shutter System (Novato, CA) and a QiClick QImaging camera (Surrey, BC, Canada).

Kinex Antibody Array. Cell lysates from HT1080 cells treated with TFP or with a DMSO control were obtained according to the protocol suggested by the Kinexus Bioinformatics Corporation (Vancouver, BC, Canada), which manufactures the Kinex antibody microarray. This assay contains over 700 antibodies against both phospho- and pan-specific antibodies. The detailed protocols can be found at the Kinexus Bioinformatics Corporation website (www.kinexus.ca).

Dual Luciferase Assay. To study β-catenin promoter activity, HT1080 cells were transiently transfected with either TOPflash or FOPflash promoter constructs (Upstate Biotechnology, Lake Placid, NY) along with the *Renilla* luciferase reporter gene using polyethylenimine (molecular weight: 250 kDa; Polysciences, Warrington, PA) after a 30-minute incubation of DNA and polyethylenimine at room temperature. Medium was changed 18 hours after transfection. Forty-eight hours after transfection and after drug treatment, luciferase activity of both firefly and *Renilla* luciferase were measured using the Promega Dual-Glo Luciferase System with the SpectraMaxL (Molecular Devices).

Transwell Migration. Transwell migration assays were performed as described previously (Dufour et al., 2008), except nuclei were stained in Hoechst/phosphate-buffered saline (PBS; 1:2000) for 20 minutes and imaged using a Nikon Eclipse TE2000-S equipped with a Sutter Instruments SmartShutter System and a QiClick QImaging camera. Migrated cells were counted with the assistance of the Nikon Elements Basic Research Software analysis tools.

Scratch Wound Migration Assay. Cells were grown to confluence in a 12-well plate and serum starved to induce cell cycle synchronization with or without TFP overnight under standard tissue culture conditions. A scratch wound was made in each well the following morning, and cells were washed twice with 1× PBS and supplemented with complete media containing drugs or vehicle. Cells were allowed to migrate over 8 hours, with bright field images being taken at time 0 and time 8 hours. Area for time 0 and time 8 hours was calculated using the Nikon Elements Basic Research Software analysis tools and percent change was calculated.

Two-Dimensional Dot Migration Assay. A collagen-cell mixture was dotted in a 96-well dish in a similar fashion to the three-dimensional invasion assay. After collagen solidification, cell-matrix dots were overlaid with complete media. Cells were allowed to migrate up to 8 hours. Cells were then stained in Hoechst/PBS (1:2000), and images were captured using the previously described microscope and camera system. Migration was then quantified by counting nuclei using the Nikon Elements Basic Research Software analysis tools.

Gelatin Zymography. Gelatin zymography was performed as described (Zucker et al., 1995). After electrophoresis, the gels were incubated in Triton X-100 to replace SDS followed by incubation in a Tris-based buffer overnight at 37°C. Staining was accomplished using Coomassie Brilliant Blue, and cleared areas were indicative of gelatinolytic activity.

Immunoblotting and Immunofluorescent Staining. Immunoblotting was done according to previously published methods and developed on a BioRad ChemiDoc (Hercules, CA) (Cao et al., 1996). Immunofluorescent staining began by fixing treated cells in 4% paraformaldehyde in PBS at 4°C, followed by permeabilization in 0.2% Triton X-100 at room temperature for 10 minutes. Blocking solution was composed of 3% bovine serum albumin/5% normal goat serum in PBS. After 1-hour blocking at room temperature, cells were exposed to anti–p-β-catenin^{Ser552} antibody (Cell Signaling Technology), visualized using the complementary secondary fluorescent antibody (anti-rabbit Alexa Fluor 568), counterstained with Hoechst, and imaged on the Nikon microscope previously described.

Knockdown of DRD2. HT1080 cells were transiently transfected with asymmetrical interfering RNA (aiRNA) directed against DRD2 (Boston Biomedical, Inc., Cambridge, MA) (Sun et al., 2008). Briefly, aiRNA and RNAiMax (Life Technologies) were incubated together at room temperature in serum-free Dulbecco's modified Eagle's medium. Transfection mixture was added to HT1080 cells and incubated overnight under standard tissue culture conditions. Four separate aiRNA were tested, and the most efficient aiRNAs were identified by real-time reverse-transcription polymerase chain reaction (RT-PCR) and chosen to complete downstream experiments.

Real-Time RT-PCR. Cellular RNA was isolated from the target cells with the Qiagen RNeasy kit (Germantown, MD). cDNA was generated using random hexamers and the iScript reverse transcriptase (BioRad). The resultant cDNA was used for real-time RT-PCR to detect DRD2 transcript levels. cDNA was subject to real-time PCR using primers generated specifically identifying DRD2 (F: 5′- CGGACAGACCCCACTACAA-3′, R: 5′- CCTGCTGAATTTCCACTCACC-3′) using the BioRad MyiQ Single-color real-time PCR thermocycler. Hypoxanthine-guanine phosphoribosyltransferase was used as a normalization control. Results were analyzed using the BioRad software MyiQ 2.0.

Statistical Analysis. Data are expressed as the standard error of the mean, and each experiment was repeated three times. Student's t test was used to determine significant differences; any $P < 0.05$ was considered significant.

Results

Identification of Compounds Capable of Inhibiting Cancer Cell Invasion. To identify small molecule compounds capable of inhibiting cancer cell invasion, a novel three-dimensional high-throughput invasion assay was used to screen the National Cancer Institute's Developmental Therapeutics Program compound library (Diversity Set II) against aggressive, androgen-independent PC3 human prostate cancer cells. This particular compound library includes 1974 compounds and covers a wide variety of chemical structures. After incubating compounds (10 μM) with PC3 cells assembled in the three-dimensional invasion assay with type I collagen in a 96-well plate for 18 hours, invaded cells were quantified based on the number of cells that were able to escape the original cell-matrix dot and invade through the adjacent cell-free collagen. The positive hits were defined as any compound that impeded 50% of invasion compared with the DMSO vehicle control. Of the 1974 compounds screened, 84 compounds were found to inhibit invasion. To segregate the inhibitory hits from potentially cytotoxic compounds, we analyzed the available half-maximal inhibitory concentration data of those positive compounds from the NCI-60 human cell line screening dataset. We defined that compounds with a half-maximal inhibitory concentration of more than 1 μM to be of interest, and 56 compounds that we identified fit within this parameter (Fig. 1A). One of the hits, TFP, is a Food and Drug Administration (FDA)–approved antipsychotic drug. Because this hit is already clinically used as a well tolerated, first line drug for patients in the acute phase of schizophrenia (Marques et al., 2004) (suggesting low systemic toxicity) and potentially has a novel function in

inhibition of cancer cell invasion, the ability of TFP to impede cancer cell invasion and the working mechanism of this drug were further evaluated.

Validating TFP as an Anti-Invasion Drug. To evaluate the potency of TFP, the dose-dependent effects of TFP on cancer cell invasion were assessed. To determine if inhibition of cancer cell invasion by TFP is not relegated to prostate cancer cells, an additional aggressive and highly invasive cancer cell line, human fibrosarcoma HT1080, was assessed. The cancer cells were assembled in a three-dimensional collagen matrix similar to the PC3 cells and exposed to increasing doses of TFP up to 10 μM. The HT1080 cells exposed to TFP demonstrated a dose-dependent decrease in invasive behavior compared with vehicle control cells (Fig. 1, B and C). We continued to use HT1080 for the remainder of these experiments because of their highly aggressive, invasive nature.

To ensure that the inhibition of invasive behavior was not due to toxicity from TFP exposure, both normal fibroblasts (murine NIH/3T3) and HT1080 cells were analyzed for chronic (repeated exposures for 3 days) toxicity in the presence of increasing doses of TFP using an MTT viability analysis. The chronic cytotoxicity assay did not show any significant cell death (Fig. 1D). Given the consideration that cells behave differently in two-dimensional culture as opposed to three-dimensional culture in response to cytotoxic agents (Peng et al., 2013), cytotoxicity of TFP was also determined in the three-dimensional culture system in the presence or absence of TFP for 24 hours, followed by imaging-based determination of cytotoxicity using PI. As negative and positive controls for cell death, cells embedded in collagen were also treated with DMSO alone or 1 μM staurosporine, an apoptosis inducer, respectively. Induction of cell death by staurosporine resulted in intense PI staining, whereas the vehicle control group displayed minimal PI-positive staining. Consistent with the two-dimensional MTT cytotoxicity assays, TFP did not cause any notable cell death in the three-dimensional milieu (Fig. 1E). Collectively these data indicate that the reduction in the invasive capacity of cancer cells observed is not a result of cell death, but rather inhibition of the drivers of invasion.

Inhibition of Cancer Cell Migration by TFP without Affecting Global Protease Activity. Cancer cell migratory ability and proteolytic activity are two critical determinants of cancer cell invasion (Friedl and Alexander, 2011). To determine which pathologic process of cell invasion is interfered with by TFP, both cell migratory ability examined by transwell migration assays and scratch wound assays and proteolytic activity examined by substrate degradation assays were assessed. PC3 cells and C4-2b cells are inhibited from migrating by TFP treatment based on transwell migration assay analyses (Fig. 2A). HT1080 cells treated with TFP had significantly reduced migratory ability compared with vehicle control (Fig. 2, B and C). Importantly, TFP had no effect on the migratory ability of the immortalized fibroblastic cell line NIH/3T3 (Fig. 2, B and C). To rule out the possibility that TFP interferes with the global proteolytic activity of the cells, a protease assay was employed to monitor enzymatic activity using a fluorescently labeled general protease substrate. The cell lysate from HT1080 cells treated with increasing doses of TFP were incubated with fluorescently labeled general protease substrate followed by analyzing substrate cleavage on a fluorescence spectrophotometer. Treatment of HT1080 cells with TFP had no significant effects on global protease activity at any dose compared with DMSO control (Fig. 2D). It has been demonstrated that HT1080 cells express a variety of matrix metalloproteinases, specifically matrix metalloproteinase (MMP)-2, -9, and -14, which have been correlated with migratory behavior (Dufour et al., 2008; Zarrabi et al., 2011). Gelatin zymography of conditioned media from HT1080 cells treated with TFP shows no changes in MMP-2 or MMP-9 gelatinolytic activity (Fig. 2E). Because MMP-14 is a physiologic activator of proMMP-2, our results suggest that TFP does not affect MMP-14 activity. Taken together, these data imply that reduction of cancer cell invasion under three-dimensional conditions by TFP is via inhibition of cell migratory ability rather than protease activity.

Effects on Angiogenesis and Basement Membrane Invasion by TFP In Vivo. Cell migration is essential to angiogenesis and invasion (Tonini et al., 2003). We next sought to determine if exposure to TFP of invasive cancer cells results in reduced angiogenesis and invasion through underlying basement membrane in vivo, by using the chicken CAM assay. HT1080 cells pretreated with TFP were adsorbed to an inert sponge and implanted on the surface of the CAM of chicken embryos. After a 4-day incubation, neovascularization induced by HT1080 cells significantly decreased in the presence of TFP compared with DMSO controls (Fig. 3, A and B). This result may be due to TFP inhibiting endothelial cell migration and/or reducing the ability of HT1080 cells to coordinate angiogenesis.

In an effort to determine the mechanism of the TFP-mediated reduction in angiogenesis, the effect of TFP on secretion of VEGF, a major soluble protein involved in vascular dynamics (Ferrara, 2004), was examined. Conditioned media from HT1080 cells treated with or without TFP were evaluated by ELISA to quantify secretion of VEGF. The conditioned media collected from HT1080 cells treated with TFP demonstrate a decreased amount of soluble VEGF in a dose-responsive fashion (Fig. 3C). These data suggest that TFP is able to inhibit the production of VEGF, leading to a decrease in angiogenesis in vivo. To further confirm that the effects on angiogenesis were mediated through modification of the cancer cell behavior and not an effect of TFP modulating the surrounding endothelial cells directly, HUVEC were monitored for network formation when laid on solidified Matrigel in the presence or absence of TFP. HUVEC exposed to 2.5 μM TFP were not impaired in forming a network similar in morphology to vehicle-treated HUVEC (Fig. 3D), suggesting that TFP exerts its antiangiogenic effect directly on the responsive cancer cells.

To directly examine if TFP is capable of inhibition of cancer cell invasion through basement membrane in vivo, the CAM invasion assay was employed. The CAM consists of the chorionic epithelium and underlying allantoic membrane that is primarily made of type IV collagen (Ribatti et al., 2001), which simulates the basement membrane of human epithelium (LeBleu et al., 2007). Invasion of cancer cells through the epithelium and basement membrane of the upper CAM into connective tissue was examined by hematoxylin and eosin staining. DMSO-treated HT1080 cells that were loaded into 2-mm diameter plastic rings over the CAM invaded into the connective tissues through the breached basement membrane. In contrast, TFP-treated HT1080 cells failed to cross through the basement membrane. Instead, the TFP-treated cells only grew on the top of the CAM (Fig. 3E). This reduction in invasion, along with the decrease in angiogenesis, suggests that TFP is effective at inhibiting invasion in vivo.

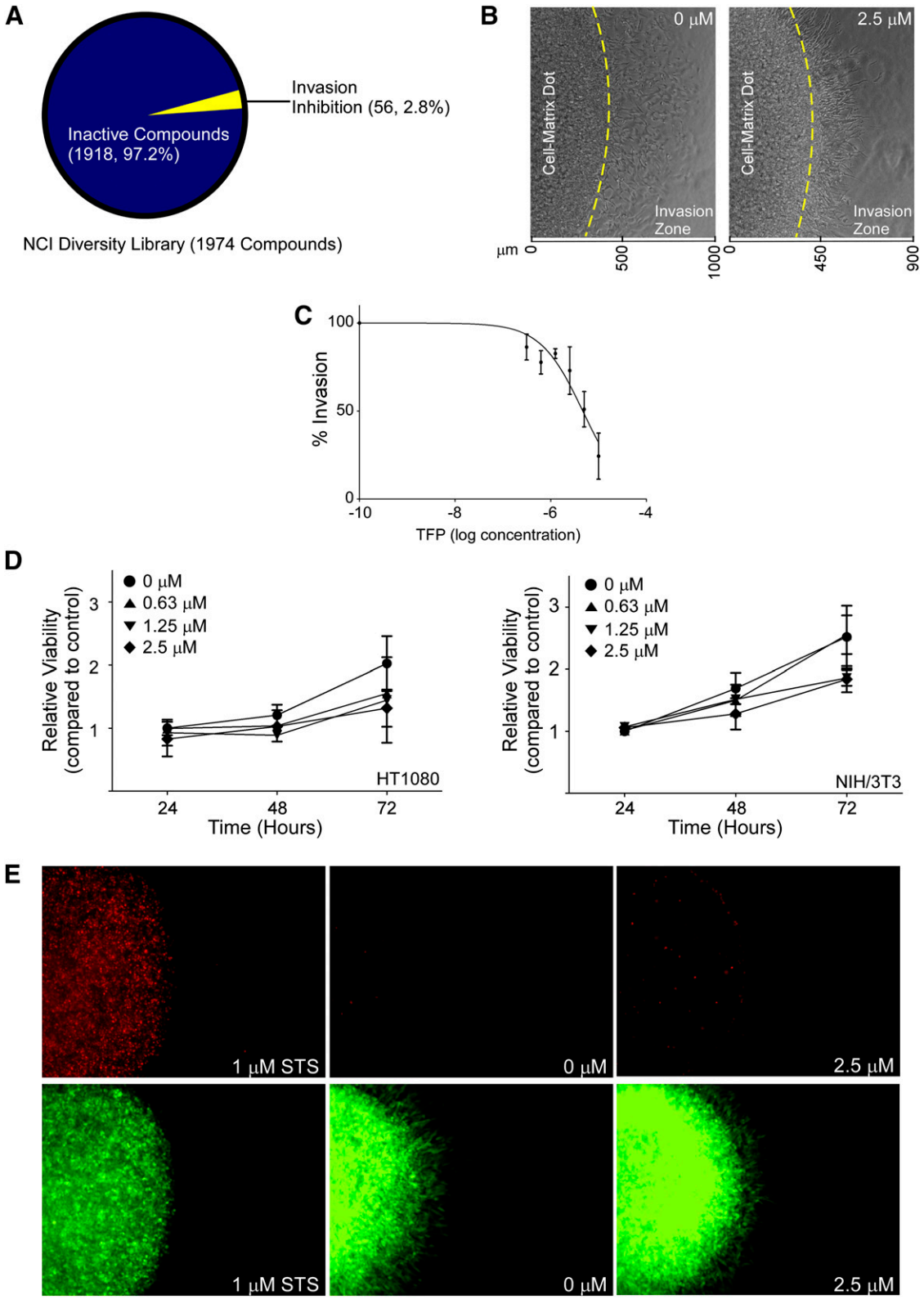

Fig. 1. Identification of the new role of TFP on inhibition of cancer cell invasion. (A) Classification of the compound library according to anti-invasive ability. Of the 1974 compounds assessed, 56 compounds were found to inhibit cancer cell invasion at 10 μM concentration. (B) Representative bright field images of HT1080 cells in a three-dimensional invasion assay demonstrates TFP reduces cell invasion at 2.5 μM concentration compared with vehicle control. Cells in the invasion zone were compared. (C) Dose dependent inhibition of HT1080 cell invasion examined by the three-dimensional invasion assay in the presence of different doses of TFP for 18 hours. (D) No significant effect by TFP on HT1080 (left panel) and NIH/3T3 (right panel) cell growth examined in a two-dimensional platform by MTT assay in the presence of different concentrations of TFP up to 72 hours. (E) TFP at 2.5 μM concentration does not cause HT1080 cell death as examined by propidium iodide staining in the three-dimensional invasion assay. Staurosporine (STS) serves as a positive control for cell death.

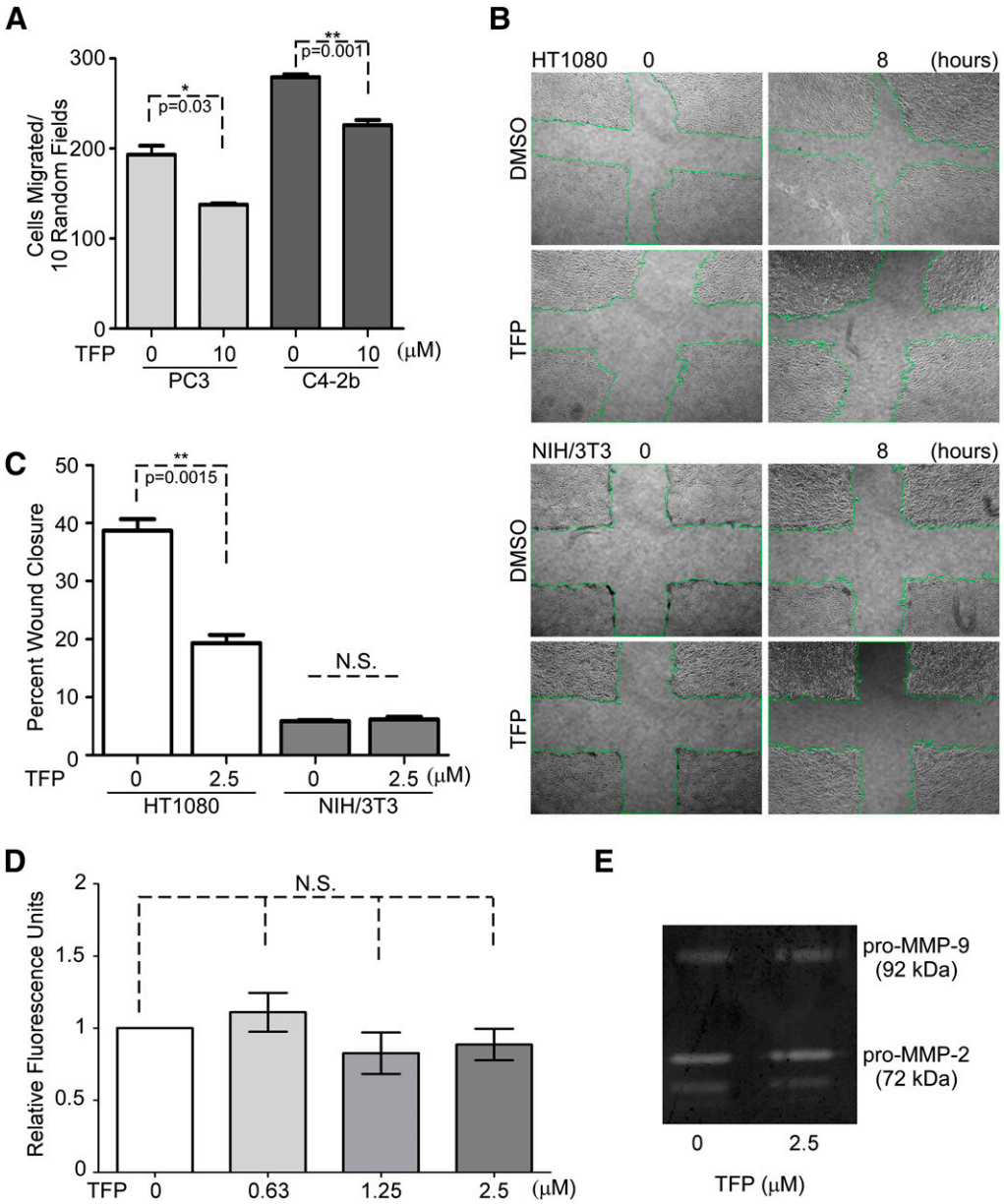

Fig. 2. TFP inhibits cell migration without affecting protease activity. (A) Transwell migration assays reveal inhibition of cancer cell migration among PC3 cells and C4-2b by TFP at 10 μM concentration. (B and C) Treatment of HT1080 cells with TFP results in a significant decrease in cell migration based on wound healing analysis, while exhibiting no effect by TFP on NIH/3T3 wound closure. NIS-Elements imaging software was used for wound closure analysis. Representative images are shown. (D) TFP has no effect on HT1080 cell proteolytic activities as examined by a fluorescent substrate degradation assay. (E) TFP treatment of HT1080 cells does not influence the expression of MMP-2 and MMP-9 and does not influence the activation of either of the gelatinases as observed in gelatin zymography.

Dissection of the Mechanism of TFP-Inhibited Cell Migration via a Cascade of DRD2, AKT, and β-Catenin. To aid in determining the molecular mechanism by which TFP reduces cancer cell invasive ability, antibody microarrays (Kinexus Bioinformatics Corporation) were employed using HT1080 cells treated with or without TFP. These arrays simultaneously detected the presence and relative quantities of over 500 pan-specific and over 300 phospho-site-specific antibodies. The data from the antibody array were analyzed using the DAVID bioinformatics program (Huang et al., 2009a,b). Input of the top hits from the antibody array into the DAVID program identified potential pathways involved, including the focal adhesion kinase pathway and the β-catenin pathway. Given the ability of each of these pathways to influence cell migration, we attempted to validate each pathway to determine the mechanism of action of TFP in inhibition of cancer cell migration. Upon further analysis, we found that treatment with TFP reduces the phosphorylation of β-catenin at Ser^{552} in HT1080 cells, whereas NIH/3T3 cells, which do not respond to TFP treatment in terms of cell migratory ability, exhibit no change in p-β-$catenin^{Ser552}$ (Fig. 4A). Ser^{552} phosphorylation of β-catenin is associated with β-catenin stabilization and subsequent translocation to the nucleus for transcription of downstream targets, some of which are associated with invasive behavior and angiogenesis (Zhang et al., 2001; Fang et al., 2007). Accordingly, immunofluorescent staining of HT1080 cells with

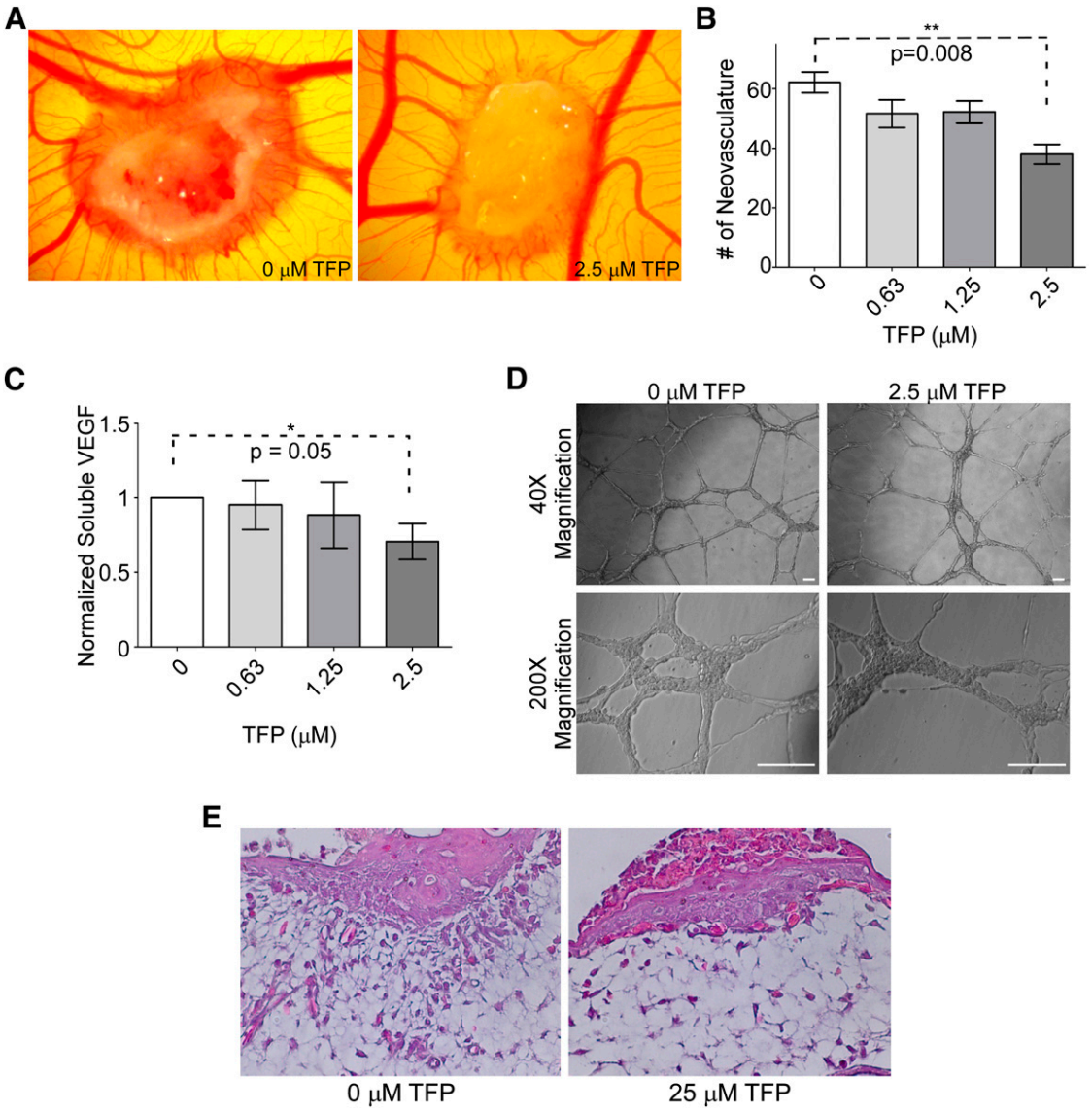

Fig. 3. TFP reduces angiogenesis and invasion examined by a chicken CAM assay. (A) Representative image of a CAM assay demonstrates that treatment of HT1080 cells with TFP reduces the ability of those cells to induce angiogenesis. (B) Quantification of neovasculature induced by HT1080 cells in the CAM assay; 2.5 μM treatment results in a significant decrease in angiogenesis. (C) TFP treatment reduces soluble VEGF. HT1080 cells treated with various doses of TFP demonstrate a reduction in VEGF expression as determined by VEGF ELISA. (D) TFP treatment does not induce changes in HUVEC network formation on a three-dimensional Matrigel platform. HUVEC cells treated with 2.5 μM TFP do not have impaired network formation or change in morphology compared with the vehicle-treated endothelial cells. Bar = 100 μm. (E) Hematoxylin and eosin staining of a tissue section collected from the CAM assay shows that HT1080 cells implanted on the CAM surface can invade through the underlying membrane, whereas TFP treatment reduces the ability of these cells to invade but continue to grow.

anti–p-Ser^{552}-β-catenin antibody resulted in significant nuclear staining of p-β-catenin in HT1080 cells treated with DMSO control. In contrast, HT1080 cells treated with TFP displayed decreased p-Ser^{552}-β-catenin in the cytoplasm and nucleus (Fig. 4D). This decreased phosphorylated β-catenin was accompanied by reduced β-catenin activity examined by a TOPflash reporter luciferase assay (Fig. 4B).

Because active AKT has been reported to phosphorylate β-catenin at Ser^{552} for nuclear translocation and subsequent interaction with the T-cell factor and lymphocyte enhancer factor transcription factors (Fang et al., 2007), AKT phosphorylation at Ser^{473} and Thr^{308} was examined by Western blotting using anti–p-AKT^{Ser473} and anti–p-AKT^{Thr308} antibodies, respectively. When HT1080 cells were treated with TFP for 24 hours, AKT phosphorylation at both phospho-sites was decreased, suggesting that TFP may suppress activity of AKT and therefore was unable to activate β-catenin through its kinase activity (Fig. 4C).

TFP effectiveness as an antipsychotic drug derives from its ability to abrogate dopamine receptor D2 (DRD2) activity (Marques et al., 2004). To determine if TFP-reduced cell migration is working through DRD2, we first surveyed DRD2 expression in cell lines that differentially respond to TFP treatment. Employing a real-time RT-PCR approach, we observed that HT1080 cells demonstrate higher expression of DRD2 compared with NIH/3T3 cells (Fig. 5A). Interestingly, NIH/3T3 cells do not respond to TFP treatment in terms of inhibition of cell migration (Fig. 2A). To further extend and

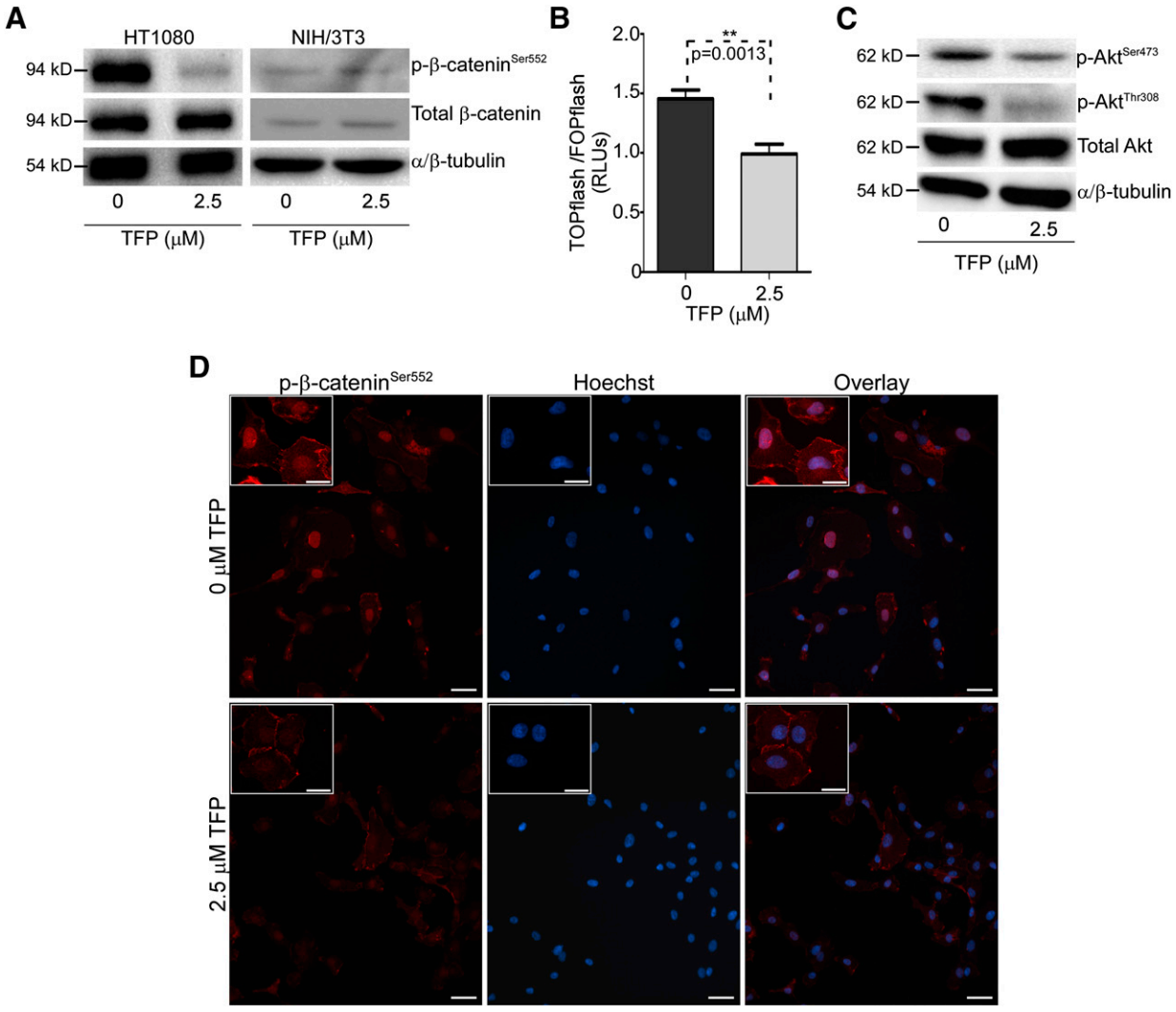

Fig. 4. TFP treatment of HT1080 cells results in a decrease in phosphorylated β-catenin^{Ser552}, AKT^{Ser473}, and AKT^{Thr308}. (A) Western blot analysis of HT1080 lysates shows that TFP treatment results in a decrease in p-β-catenin^{Ser552}, whereas there are no changes in TFP-treated NIH/3T3 cells. Total β-catenin and α/β tubulin were used as controls. (B) TFP treatment of HT1080 cells reduces the transcriptional activity of β-catenin as assessed by TOPflash/FOPflash luciferase activity, expressed in relative luciferase units (RLUs). (C) Decreases of phosphorylated AKT in HT1080 cells treated with TFP (2.5 μM) for 18 hours examined by Western blot using antiphospho-AKT^{Ser473} and AKT^{Thr308} antibodies, respectively. Total AKT and α/β-tubulin were used as controls. (D) Immunofluorescent staining of HT1080 cells treated with TFP shows decreased nuclear p-β-catenin^{Ser552} staining compared with vehicle control using anti–phospho-β-catenin antibody. Nuclei were stained by Hoechst. β-Catenin staining and nuclear staining were superimposed (overlay) Bar = 50 μm. Enlarged representative images are shown in the inserts. Bar = 20 μm.

determine whether inhibition of cell migration by TFP is through antagonistic effects on DRD2, we used an aiRNA interference approach (Sun et al., 2008) to downregulate DRD2 expression in HT1080 cells. Effective downregulation of DRD2, achieved using DRD2 aiRNA in HT1080 cells, was demonstrated both at the mRNA and protein levels (Fig. 5, B and C). By the functional study in terms of cell migration, silencing DRD2 in HT1080 cells results in a decrease in cell migration compared with controls (Fig. 5F). Because TFP affects protein phosphorylation status of β-catenin^{Ser552} and AKT^{Thr308} (Fig. 4, A and C), we additionally measured protein phosphorylation status in DRD2-silenced cells. By Western blotting using corresponding antibodies, those HT1080 cells with knockdown of DRD2 demonstrate a reduced level of p-β-catenin^{Ser552} and p-AKT^{Thr308} (Fig. 5, D and E), further confirming that TFP-reduced cell migration is through an antagonistic effect on DRD2.

To further support the idea that DRD2 antagonism is the cause of these molecular changes, we treated HT1080 cells with haloperidol, another FDA-approved antipsychotic medication that is a known DRD2 inhibitor, followed by Western blotting analysis. Consistent with TFP treatment, cells treated with haloperidol display reduced p-β-catenin^{Ser552} (Fig. 5G). In addition, HT1080 cells treated with haloperidol demonstrated reduced migration when assessed via scratch wound, similar to those treated with TFP (Fig. 5, H and I). These data reinforce our conclusion that TFP-reduced cell migration is primarily through antagonistic effects on DRD2, whereas inhibition of alternate targets of TFP, such as calmodulin or multidrug resistance gene products, may not be the primary cause of a reduction in p-β-catenin^{Ser552}, p-AKT^{Thr308}, and p-AKT^{Ser473}. Collectively, our data shows that DRD2 is likely the direct target of TFP, and inhibition of cell migration by TFP is via a DRD2-AKT-β-catenin network that ultimately modifies migratory behavior.

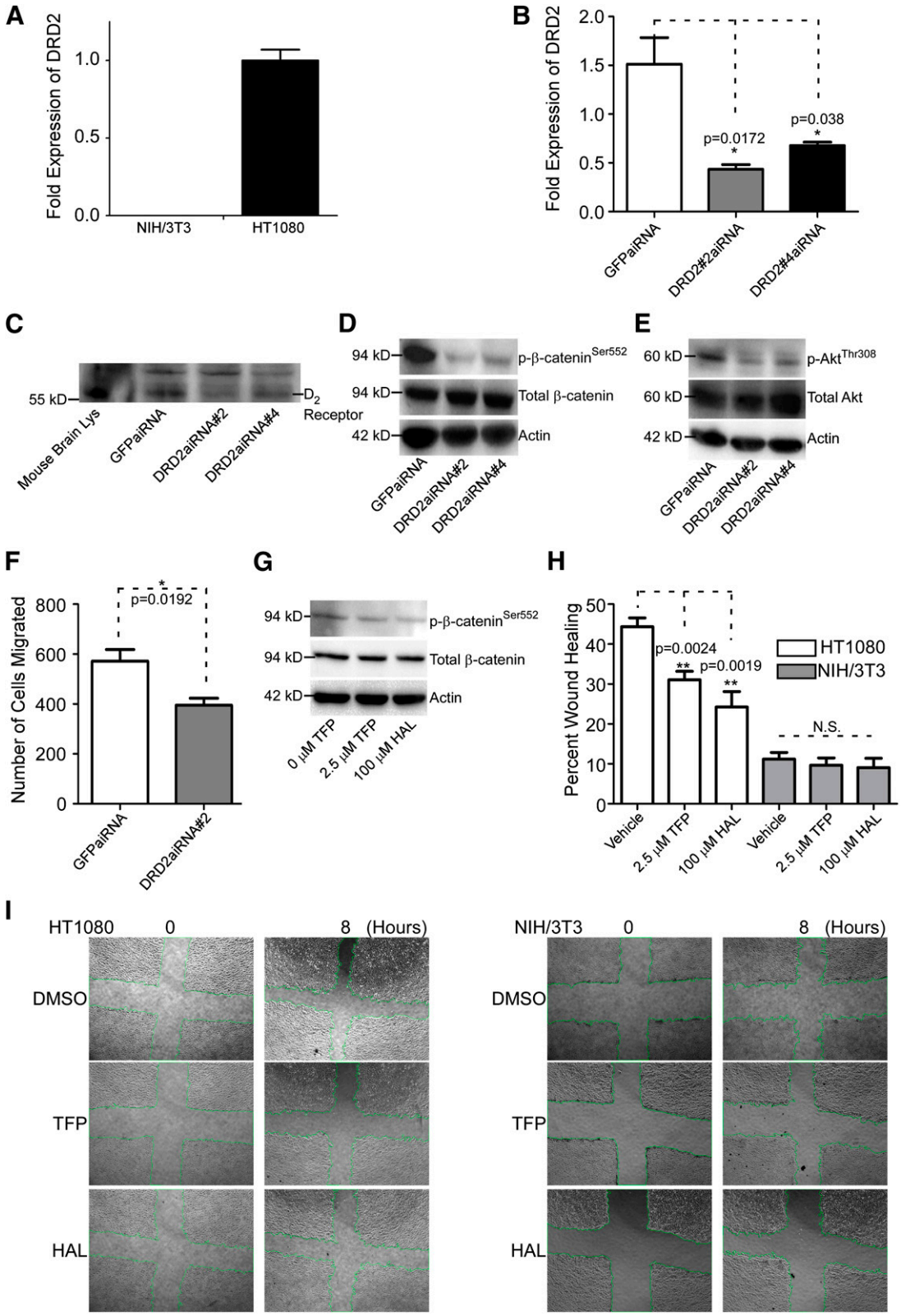

Fig. 5. Knockdown of DRD2 results in decreased phosphorylated β-catenin^{Ser552} and AKT^{Ser473} and reduced cancer cell migration. (A) Real-time RT-PCR analysis of NIH/3T3 and HT1080 cells reveals that HT1080 cells express a relatively high level of DRD2 mRNA compared with NIH/3T3. The hypoxanthine-guanine phosphoribosyltransferase (HPRT) housekeeping gene was used as a normalization control. The experiment was repeated three times. (B) Silencing of DRD2 by validated aiRNAs in HT1080 cells examined by real-time RT-PCR. The HPRT housekeeping gene was used as a normalization control. The experiment was repeated three times. (C) aiRNA knockdown of DRD2 results in less DRD2 expression examined by Western blot using an anti-DRD2 antibody. Mouse brain lysate was used as a positive control and nonspecific bands were used as loading control. (D) Knockdown of DRD2 results in decreased p-β-catenin^{Ser552} as demonstrated by Western blot analysis using an anti–p-β-catenin^{Ser552} antibody. Total β-catenin and β-actin were used as controls. (E) p-AKT^{Thr308} is reduced when DRD2 is knocked down in HT1080 cells examined by Western blotting

Discussion

Unlike conventional high-throughput screening assays for anticancer invasion drug discovery that used biochemical assays for targeting proteolytic activity or various two-dimensional migration assays for targeting cancer cell migratory machinery, our unbiased three-dimensional screening platform has the capacity to mimic in vivo conditions of cancer invasion for identification of compounds that efficiently inhibit cancer cell invasion. Using this novel three-dimensional high-throughput invasion assay, we identified TFP, an FDA-approved antipsychotic drug, which was efficient at attenuating cancer cell invasion through a DRD2-AKT-β-catenin network without causing significant cell death, as a drug for preventing cancer metastasis. Our data highlight a new potential treatment strategy by use of an old drug against cancer progression.

The cancer drug discovery process has traditionally focused on identifying cytotoxic agents in lieu of compounds that reduce the mobile phenotype of invasive cancer cells. Although highly effective in some hematologic malignancies, the tumor-shrinkage paradigm is not curative for most advanced solid cancers. This important point indicates that a phenotype-based screening program targeting cancer invasion has the potential to yield effective, less-toxic drugs. By using the high-throughput three-dimensional invasion assay developed in our laboratory (Evensen et al., 2013), Diversity Set II from the National Cancer Institute collection was screened for compounds that target cancer cell invasion, a critical determinant of cancer metastasis. On the basis of our initial screening, TFP is found to be effective at reducing invasion without notable cytotoxicity, as evidenced not only by the in vitro data presented here but also by its wide clinical use and tolerable side effects.

Our findings may have implications for a novel treatment strategy in patients with cancer. Not only is TFP safe when administered alone to patients, but it has been shown to be safe in combination with some traditional chemotherapies and may even potentiate the cytotoxic actions of these therapies (Sullivan et al., 2002; Zhelev et al., 2004; Polischouk et al., 2007; Sangodkar et al., 2012). We currently propose that TFP is a valuable tool specifically for prevention of metastases. In support of this idea, a retrospective study indicates that cancer patients incidentally taking calcium channel antagonists, including TFP, for several months during their treatments had delayed disease progression and increased survival rates (Zacharski et al., 1990). The work presented here suggests that TFP has great potential because of its ability to reduce cancer cell invasion and tumor angiogenesis as a single agent, not necessarily related to potentiating chemotherapeutic effects or reversal of multidrug resistance or calmodulin inhibition.

The angiogenesis data presented here demonstrate that TFP can have far-reaching effects, even in an in vivo context. Treatment of HT1080 cells with TFP reduced their angiogenic potential, demonstrated by the significant decrease in neovascularization and reduction in VEGF production. This reduction is likely not due to an effect on the surrounding endothelial cells, as demonstrated by the network of HUVEC cells that form in the presence or absence of TFP, indicating that the endothelial cells are not directly responding to TFP but are responding to the changing signals from TFP-treated HT1080 cells.

Our use of 25 μM concentration of TFP for the in vivo invasion assay utilizing the CAM is justified in that the volume that contained TFP and tumor cells was small compared with the volume of the entire chicken embryo and there is an assumption that diffusion through the fluids in the chicken embryo reduces local concentrations of TFP during a 4-day incubation period. Furthermore, the TFP concentration in the CAM assay shows no sign of cytotoxicity, because there is a mass of cells that grow atop the basement membrane during the length of the experiment even with higher concentration TFP exposure. Finally, there are reports that identify patient plasma levels of TFP in the range of 2–36 μM (Zhelev et al., 2004), placing our chosen higher concentration within a clinically relevant range.

Previous studies have demonstrated that the effects of TFP on neurologic diseases are via antagonism of DRD2 (Marques et al., 2004). We postulate based on the data herein that the reduction in phosphorylated β-catenin and AKT is a result of inhibition of DRD2. DRD2 is a seven transmembrane domain, G-protein–coupled receptor that is highly expressed in certain parts of the central nervous system, particularly the striatum, and in vasculature and the retina among other organs (Beaulieu and Gainetdinov, 2011). Over the past several years, evidence that dopamine receptors are expressed in cancer cells outside the nervous system has been increasing. DRD2 expression has been found in abnormally proliferating Jurkat cells, prostate cancer lines (LnCAP), and lung cancer stem cells (Arvigo et al., 2010; Basu et al., 2010; Yeh et al., 2012).

Our data specifically indicate that TFP treatment of HT1080 cells leads to a decrease in phosphorylated β-catenin. Not only does inhibition of DRD2 result in this decrease, but knockdown of DRD2 in HT1080 cells recapitulates the molecular phenotype of TFP treatment. Furthermore, we demonstrated that β-catenin inhibition by TFP, potentially via inhibition of AKT, results in a decrease in β-catenin transcriptional activity and therefore a downregulation of downstream targets, specifically VEGF. The antibody array indicated that proteins such as cyclin D1, c-met, and connexin were downregulated by TFP, which is relevant, considering these molecules have been tied to β-catenin activity (Tetsu and McCormick, 1999; Ai et al., 2000; Boon et al., 2002).

The phenotype assessed in this work, namely cancer cell invasion, can be considerably influenced by β-catenin activity. Several past reports have associated β-catenin activity with enhanced cell migration and invasion, primarily by upregulation of molecules that initiate the epithelial-to-mesenchymal

using anti–p-AKT^{Thr308} antibody. Total AKT and actin were used as controls. (F) Knockdown of DRD2 results in reduced cancer cell migration in HT1080 cells examined by a two-dimensional dot cell migration assay. (G) Haloperidol, as well as TFP reduced p-β-catenin^{Ser552}, examined by Western blotting analysis using an anti–p-β-catenin^{Ser552} antibody. Total β-catenin and β-actin were used as controls. (H) TFP and haloperidol decrease HT1080 cell migration as demonstrated by a wound healing migration assay. There are no effects on NIH/3T3 cells. The experiment was repeated three times. (I) Representative images of wound healing in HT1080 and NIH/3T3 untreated, TFP-treated, and haloperidol-treated cells. GFP, green fluorescent protein; HAL, haloperidol; Lys, lysate.

transition (EMT), a contributing factor to the initial cell invasion step of metastasis (Thakur and Mishra, 2013). ZEB1, Twist1, and Brachyury are all examples of EMT-associated transcription factors that are direct targets of β-catenin (Arnold et al., 2000; Howe et al., 2003; Fernando et al., 2010; Sanchez-Tillo et al., 2011). These transcription factors have all been associated with a reduction in epithelial characteristics, such as a loss of E-cadherin, and an increase in mesenchymal features, such as an increase in the intermediate filament vimentin (Yang et al., 2004; Aigner et al., 2007; Fernando et al., 2010). Ultimately, reducing the stability of β-catenin can exert a great effect on the ability of cells to become motile due to the relationship between β-catenin activity and an increase in EMT. Although β-catenin is a crucial molecule to cancer development and progression, this protein has traditionally been considered difficult to target because of the nature of its interacting site participating in several different interactions (Takada et al., 2012). A number of recent reports focused on identifying specific β-catenin inhibitors, with various strategies being taken to effectively and specifically disrupt β-catenin signaling.

Interfering with β-catenin activity can also reduce products such as IL-10 that influence the ability of cancer cells to act in an immunosuppressive fashion (Yaguchi et al., 2012). Additionally, it has been reported that cancer stem-like cells (CSCs) rely on the β-catenin pathway for self-renewal (Hsieh et al., 2013); because this particular cell type found in the heterogeneous milieu of tumors is thought to be responsible for cancer metastasis and relapse, it would be beneficial to target the pathways on which it is reliant. A recent publication that focused on lung CSCs found that TFP treatment results in a decrease in the β-catenin pathway and loss of some stem-like phenotypes (Yeh et al., 2012). In additional support of our findings here, a screening of compounds by Sachlos et al. (2012) to identify anti-CSC therapies revealed that dopamine receptors are found on CSC surfaces, as well as patient breast cancer cells, and antipsychotic drugs may be promising avenues of treatment. Therefore, there exists potential for agents such as TFP that reduce β-catenin target gene products to influence multiple aspects of cancer cell biology, including migration and invasion, angiogenesis, local immunosuppression, and reduction in clonogenic CSCs. Because the Wnt/β-catenin pathway is frequently dysregulated in cancer and mediates some cancer stem cell-like properties, it is desirable to inhibit this pathway (Barker and Clevers, 2006; Takahashi-Yanaga and Kahn, 2010). The ability of TFP to inhibit β-catenin signaling is valuable for a broad spectrum of cancers. We have shown that cancer cell lines of various lineages have functional responses to TFP, specifically those of fibrosarcoma and prostate origin.

Our observation of this old drug as an anti-invasive agent opens up the possibility of using an FDA-approved, clinically used drug "off-label" for patients with cancer. The FDA approval associated with TFP implies that it is a safe drug to use in large populations and has tolerable or manageable side effects. It has been reported that only 5% of oncology drugs that reach clinical trials will succeed to approval, but there exists hope in improving these statistics by re-examining known drugs that might have secondary applications (for review see Gupta et al., 2013). Repurposing known small molecules is a strategy to combat the decline in introduction of new molecular entities to the market (Paul et al., 2010). Our work clearly identifies a relatively safe, known drug (TFP) as a potential anti-invasion cancer drug in addition to its traditional role as an antipsychotic.

We identified TFP as a potential novel therapeutic agent for invasion and metastasis via a reduction in phosphorylation of AKT and β-catenin, reducing target gene expression and invasive behavior. This drug has potential immediate translational value, because this compound has a relatively low cost and has been used extensively in other clinical situations. We identified the potential molecular basis for the anti-invasive activity of TFP, but based on effects on other properties of cancer cells (e.g., CSC, calcium channels), the clinical effectiveness of this type of drug use in cancer remains to be determined. Future studies are needed to determine whether the cellular and molecular changes that we demonstrated in prostate cancer and fibrosarcoma cells are recapitulated in a variety of cancer cell types.

Acknowledgments

The authors thank the laboratory of Dr. David Talmage for providing reagents and helpful suggestions regarding the dopamine receptor.

Author Contributions

Participated in research design: Pulkoski-Gross, J. Li, Cao.
Conducted experiments: Pulkoski-Gross, J. Li, Zheng, Y. Li, Ouyang.
Performed data analysis: Pulkoski-Gross, J. Li, Rigas, Zucker, Cao.
Wrote or contributed to the writing of the manuscript: Pulkoski-Gross.

References

Ai Z, Fischer A, Spray DC, Brown AM, and Fishman GI (2000) Wnt-1 regulation of connexin43 in cardiac myocytes. *J Clin Invest* **105**:161–171.
Aigner K, Dampier B, Descovich L, Mikula M, Sultan A, Schreiber M, Mikulits W, Brabletz T, Strand D, and Obrist P et al. (2007) The transcription factor ZEB1 (deltaEF1) promotes tumour cell dedifferentiation by repressing master regulators of epithelial polarity. *Oncogene* **26**:6979–6988.
Anders M, Hansen R, Ding RX, Rauen KA, Bissell MJ, and Korn WM (2003) Disruption of 3D tissue integrity facilitates adenovirus infection by deregulating the coxsackievirus and adenovirus receptor. *Proc Natl Acad Sci USA* **100**:1943–1948.
Arnold SJ, Stappert J, Bauer A, Kispert A, Herrmann BG, and Kemler R (2000) Brachyury is a target gene of the Wnt/β-catenin signaling pathway. *Mech Dev* **91**: 249–258.
Arvigo M, Gatto F, Ruscica M, Ameri P, Dozio E, Albertelli M, Culler MD, Motta M, Minuto F, and Magni P et al. (2010) Somatostatin and dopamine receptor interaction in prostate and lung cancer cell lines. *J Endocrinol* **207**:309–317.
Barker N and Clevers H (2006) Mining the Wnt pathway for cancer therapeutics. *Nat Rev Drug Discov* **5**:997–1014.
Basu B, Sarkar C, Chakroborty D, Ganguly S, Shome S, Dasgupta PS, and Basu S (2010) D1 and D2 dopamine receptor-mediated inhibition of activated normal T cell proliferation is lost in jurkat T leukemic cells. *J Biol Chem* **285**:27026–27032.
Beaulieu J-M and Gainetdinov RR (2011) The physiology, signaling, and pharmacology of dopamine receptors. *Pharmacol Rev* **63**:182–217.
Bissell MJ and Radisky D (2001) Putting tumours in context. *Nat Rev Cancer* **1**: 46–54.
Bissell MJ, Weaver VM, Lelièvre SA, Wang F, Petersen OW, and Schmeichel KL (1999) Tissue structure, nuclear organization, and gene expression in normal and malignant breast. *Cancer Res* **59**(7, Suppl)1757–1764s.
Boon EM, van der Neut R, van de Wetering M, Clevers H, and Pals ST (2002) Wnt signaling regulates expression of the receptor tyrosine kinase met in colorectal cancer. *Cancer Res* **62**:5126–5128.
Cao J, Rehemtulla A, Bahou W, and Zucker S (1996) Membrane type matrix metalloproteinase 1 activates pro-gelatinase A without furin cleavage of the N-terminal domain. *J Biol Chem* **271**:30174–30180.
Comen E and Norton L (2012) Self-seeding in cancer. *Recent Results Cancer Res* **195**: 13–23.
Deryugina EI and Quigley JP (2008) Chick embryo chorioallantoic membrane model systems to study and visualize human tumor cell metastasis. *Histochem Cell Biol* **130**:1119–1130.
Dufour A, Sampson NS, Zucker S, and Cao J (2008) Role of the hemopexin domain of matrix metalloproteinases in cell migration. *J Cell Physiol* **217**:643–651.
Evensen NA, Li J, Yang J, Yu X, Sampson NS, Zucker S, and Cao J (2013) Development of a high-throughput three-dimensional invasion assay for anti-cancer drug discovery. *PLoS ONE* **8**:e82811.
Fang D, Hawke D, Zheng Y, Xia Y, Meisenhelder J, Nika H, Mills GB, Kobayashi R, Hunter T, and Lu Z (2007) Phosphorylation of β-catenin by AKT promotes β-catenin transcriptional activity. *J Biol Chem* **282**:11221–11229.
Fernando RI, Litzinger M, Trono P, Hamilton DH, Schlom J, and Palena C (2010) The T-box transcription factor Brachyury promotes epithelial-mesenchymal transition in human tumor cells. *J Clin Invest* **120**:533–544.

Ferrara N (2004) Vascular endothelial growth factor: basic science and clinical progress. *Endocr Rev* **25**:581–611.
Friedl P and Alexander S (2011) Cancer invasion and the microenvironment: plasticity and reciprocity. *Cell* **147**:992–1009.
Gupta SC, Sung B, Prasad S, Webb LJ, and Aggarwal BB (2013) Cancer drug discovery by repurposing: teaching new tricks to old dogs. *Trends Pharmacol Sci* **34**: 508–517.
Hanahan D and Weinberg RA (2011) Hallmarks of cancer: the next generation. *Cell* **144**:646–674.
Horning JL, Sahoo SK, Vijayaraghavalu S, Dimitrijevic S, Vasir JK, Jain TK, Panda AK, and Labhasetwar V (2008) 3-D tumor model for in vitro evaluation of anticancer drugs. *Mol Pharm* **5**:849–862.
Howe LR, Watanabe O, Leonard J, and Brown AM (2003) Twist is up-regulated in response to Wnt1 and inhibits mouse mammary cell differentiation. *Cancer Res* **63**: 1906–1913.
Hsieh CH, Chao KS, Liao HF, and Chen YJ (2013) Norcantharidin, derivative of cantharidin, for cancer stem cells. *Evid Based Complement Alternat Med* **2013**: 838651.
Huang W, Sherman BT, and Lempicki RA (2009a) Bioinformatics enrichment tools: paths toward the comprehensive functional analysis of large gene lists. *Nucleic Acids Res* **37**:1–13.
Huang W, Sherman BT, and Lempicki RA (2009b) Systematic and integrative analysis of large gene lists using DAVID bioinformatics resources. *Nat Protoc* **4**: 44–57.
Kim MY, Oskarsson T, Acharyya S, Nguyen DX, Zhang XH, Norton L, and Massagué J (2009) Tumor self-seeding by circulating cancer cells. *Cell* **139**:1315–1326.
Leaf C and Burke D (2004) Why We're Losing The War On Cancer [And How To Win It]. *Fortune* **145**:1.
LeBleu VS, Macdonald B, and Kalluri R (2007) Structure and function of basement membranes. *Exp Biol Med (Maywood)* **232**:1121–1129.
Marques LO, Lima MS, and Soares BG (2004) Trifluoperazine for schizophrenia. *Cochrane Database Syst Rev* (1):CD003545.
Norton L and Massagué J (2006) Is cancer a disease of self-seeding? *Nat Med* **12**: 875–878.
Paul SM, Mytelka DS, Dunwiddie CT, Persinger CC, Munos BH, Lindborg SR, and Schacht AL (2010) How to improve R&D productivity: the pharmaceutical industry's grand challenge. *Nat Rev Drug Discov* **9**:203–214.
Peng CC, Chyau CC, Wang HE, Chang CH, Chen KC, Chou KY, and Peng RY (2013) Cytotoxicity of ferulic Acid on T24 cell line differentiated by different microenvironments. *Biomed Res Int* **2013**:579859.
Polischouk AG, Holgersson A, Zong D, Stenerlöw B, Karlsson HL, Möller L, Viktorsson K, and Lewensohn R (2007) The antipsychotic drug trifluoperazine inhibits DNA repair and sensitizes non small cell lung carcinoma cells to DNA double-strand break induced cell death. *Mol Cancer Ther* **6**:2303–2309.
Redig AJ and McAllister SS (2013) Breast cancer as a systemic disease: a view of metastasis. *J Intern Med* **274**:113–126.
Ribatti D, Nico B, Vacca A, and Presta M (2006) The gelatin sponge-chorioallantoic membrane assay. *Nat Protoc* **1**:85–91.
Ribatti D, Nico B, Vacca A, Roncali L, Burri PH, and Djonov V (2001) Chorioallantoic membrane capillary bed: a useful target for studying angiogenesis and anti-angiogenesis in vivo. *Anat Rec* **264**:317–324.
Sachlos E, Risueño RM, Laronde S, Shapovalova Z, Lee JH, Russell J, Malig M, McNicol JD, Fiebig-Comyn A, and Graham M et al. (2012) Identification of drugs including a dopamine receptor antagonist that selectively target cancer stem cells. *Cell* **149**:1284–1297.
Sánchez-Tilló E, de Barrios O, Siles L, Cuatrecasas M, Castells A, and Postigo A (2011) β-catenin/TCF4 complex induces the epithelial-to-mesenchymal transition (EMT)-activator ZEB1 to regulate tumor invasiveness. *Proc Natl Acad Sci USA* **108**:19204–19209.
Sangodkar J, Dhawan NS, Melville H, Singh VJ, Yuan E, Rana H, Izadmehr S, Farrington C, Mazhar S, and Katz S et al. (2012) Targeting the FOXO1/KLF6 axis regulates EGFR signaling and treatment response. *J Clin Invest* **122**:2637–2651.
Sullivan GF, Garcia-Welch A, White E, Lutzker S, and Hait WN (2002) Augmentation of apoptosis by the combination of bleomycin with trifluoperazine in the presence of mutant p53. *J Exp Ther Oncol* **2**:19–26.
Sun X, Rogoff HA, and Li CJ (2008) Asymmetric RNA duplexes mediate RNA interference in mammalian cells. *Nat Biotechnol* **26**:1379–1382.
Takada K, Zhu D, Bird GH, Sukhdeo K, Zhao JJ, Mani M, Lemieux M, Carrasco DE, Ryan J, and Horst D et al. (2012) Targeted disruption of the BCL9/beta-catenin complex inhibits oncogenic Wnt signaling. *Sci Transl Med* **4**: 148ra117.
Takahashi-Yanaga F and Kahn M (2010) Targeting Wnt signaling: can we safely eradicate cancer stem cells? *Clin Cancer Res* **16**:3153–3162.
Talmadge JE and Fidler IJ (2010) AACR centennial series: the biology of cancer metastasis: historical perspective. *Cancer Res* **70**:5649–5669.
Tetsu O and McCormick F (1999) Beta-catenin regulates expression of cyclin D1 in colon carcinoma cells. *Nature* **398**:422–426.
Thakur R and Mishra DP (2013) Pharmacological modulation of beta-catenin and its applications in cancer therapy. *J Cell Mol Med* **17**:449–456.
Tonini T, Rossi F, and Claudio PP (2003) Molecular basis of angiogenesis and cancer. *Oncogene* **22**:6549–6556.
Yaguchi T, Goto Y, Kido K, Mochimaru H, Sakurai T, Tsukamoto N, Kudo-Saito C, Fujita T, Sumimoto H, and Kawakami Y (2012) Immune suppression and resistance mediated by constitutive activation of Wnt/β-catenin signaling in human melanoma cells. *J Immunol* **189**:2110–2117.
Yang J, Mani SA, Donaher JL, Ramaswamy S, Itzykson RA, Come C, Savagner P, Gitelman I, Richardson A, and Weinberg RA (2004) Twist, a master regulator of morphogenesis, plays an essential role in tumor metastasis. *Cell* **117**:927–939.
Yeh C-T, Wu ATH, Chang PM-H, Chen K-Y, Yang C-N, Yang S-C, Ho C-C, Chen C-C, Kuo Y-L, and Lee P-Y et al. (2012) Trifluoperazine, an antipsychotic agent, inhibits cancer stem cell growth and overcomes drug resistance of lung cancer. *Am J Respir Crit Care Med* **186**:1180–1188.
Zacharski LR, Moritz TE, Haakenson CM, O'Donnell JF, Ballard HS, Johnson GJ, Ringenberg QS, Schilsky RL, Spaulding MB, and Tornyos K et al. (1990) Chronic calcium antagonist use in carcinoma of the lung and colon: a retrospective cohort observational study. *Cancer Invest* **8**:451–458.
Zarrabi K, Dufour A, Li J, Kuscu C, Pulkoski-Gross A, Zhi J, Hu Y, Sampson NS, Zucker S, and Cao J (2011) Inhibition of matrix metalloproteinase 14 (MMP-14)-mediated cancer cell migration. *J Biol Chem* **286**:33167–33177.
Zhang X, Gaspard JP, and Chung DC (2001) Regulation of vascular endothelial growth factor by the Wnt and K-ras pathways in colonic neoplasia. *Cancer Res* **61**: 6050–6054.
Zhelev Z, Ohba H, Bakalova R, Hadjimitova V, Ishikawa M, Shinohara Y, and Baba Y (2004) Phenothiazines suppress proliferation and induce apoptosis in cultured leukemic cells without any influence on the viability of normal lymphocytes. Phenothiazines and leukemia. *Cancer Chemother Pharmacol* **53**:267–275.
Zucker S, Conner C, DiMassmo BI, Ende H, Drews M, Seiki M, and Bahou WF (1995) Thrombin induces the activation of progelatinase A in vascular endothelial cells. Physiologic regulation of angiogenesis. *J Biol Chem* **270**:23730–23738.

Address correspondence to: Dr. Jian Cao, Dept of Medicine/Cancer Prevention, Stony Brook University, Stony Brook, NY. E-mail: jian.cao@sunysb.edu